JOC Article

Solution-State Conformational Study of the Hevamine Inhibitor Allosamidin and Six Potential Inhibitor Analogues by NMR Spectroscopy and Molecular Modeling

Antje Germer, Martin G. Peter, and Erich Kleinpeter*

Institut für Organische Chemie und Strukturanalytik, Universität Potsdam, Am Neuen Palais 10, D-14469 Potsdam, FR Germany

kp@chem.uni-potsdam.de

Received December 13, 2001

The solution-state conformations of the hevamine inhibitor allosamidin and six potential inhibitor analogues were studied by various NMR spectroscopic techniques and molecular modeling using force field calculations. Determination solely of the global energy minimum conformation was found to be insufficient for consensus with the NMR results, and agreement between the NMR experimental data and the theoretical calculations was only reached by assessing the structures as population-weighted average conformers on the basis of Boltzmann distributions derived from the calculated relative energies. The conformations of the glycosidic linkages in the compounds were found to be similar when the sugar residues were the same, but differences were markedly evident otherwise and also for the various heterocyclic group linkages. The binding of the compounds to hevamine, which may also complex to chitinases in general, was assessed using HMQC, transfer-NOESY, and both 1-D and 2-D saturation transfer difference NMR experiments. Under the conditions employed, only allosamidin was implicated to be bound to hevamine, and then only by HMQC with the dipolar coupling-based experiments failing to substantiate the formation of the complex. However, the results are consistent with the biochemical activities of the compounds whereby only allosamidin has been shown to act as a competitive inhibitor.

Introduction

Chitinases, e.g., hevamine, are enzymes that cleave the bond between two consecutive *N*-acetylglucosamine residues of chitin. Since these enzymes play a key role in nature as plant biocontrol agents against fungal elicitors, they are of prime biotechnological importance. Chitinase inhibitors are also potential insecticides and fungicides. To design novel potential inhibitors rationally, a complete understanding of the underlying molecular mechanisms of the interaction of chitinases with oligosaccharide substrates is essential. This requires the application of experimental and theoretical techniques that characterize the structure and dynamics of oligosaccharides and their complexes with the enzyme.

NMR spectroscopy repeatedly has proven to be the method of choice for assessing the adopted conformation of oligosaccharides in aqueous solution.[1] The limiting problem in determining the solution conformation, however, is the high flexibility of these oligosaccharides, and therefore, it is necessary to engage computational methods to assist in the interpretation of the NMR data. Specific NOE contacts, as well as coupling constants, corresponding to a particular conformation are only interpretable in that form if this conformation is highly populated in solution and since oligosaccharides usually populate several conformations at ambient temperature,[2] observed NOE contacts (and coupling constants) represent a population-weighted average of all participating conformations. Therefore, population-weighted average internuclei distances have to be calculated first for the complete number of accessible conformations before assessment of the experimentally observed NOEs can be made.[3] The primary objective of this work was to study the structure, stereochemistry, and conformational behavior of allosamidin (**1**) and some recently synthesized analogues,[4,5] **2**−**7** (see Figure 1), in the solution state by NMR spectroscopic techniques and molecular modeling using force field calculations. In comparison to the naturally occurring potent inhibitor allosamidin (**1**), the variations present in the analogues include the following: changing the sugar units from *N*-acetylallosamine to *N*-acetylglucosamine (**2**−**7**); changing the heterocyclic moiety (**2**−**4**), replacing it by an acyclic heteroatom-containing chain (**6**−**7**), or dispensing with it altogether (**5**); or introducing a succinamide spacer group between the two sugar units (**5** and **6**). This latter pair also bears

* To whom correspondence should be addressed. Phone: 49-(331)-977-5210. Fax: 49-(331)-977-5064.

(1) Peters, T.; Pinto, B. M. *Curr. Opin. Struct. Biol.* **1996**, *6*, 710.

(2) Cumming, D. A.; Carver, J. P. *Biochemistry* **1987**, *26*, 6664.

(3) Carver, J. P.; Mandel, D.; Michnick, S. W.; Imberty A.; Brady, J. W. In *Computer Modeling of Carbohydrate Molecules*; French A. D., Brady J. W., Eds.; ACS Symposium Series 430; American Chemical Society: Washington, DC, 1990; p 266.

(4) Rottmann, A.; Synstad, B.; Eijsink, V.; Peter, M. G. *Eur. J. Org. Chem.* **1999**, 2293.

(5) Thiele, G.; Rottmann, A.; Germer, A.; Kleinpeter, E.; Spindler, K.-D.; Eijsink, V. G. H.; Peter, M. G. *J. Carbohydr. Chem.* **2001**, in press.

10.1021/jo0163703 CCC: $22.00
Published on Web 08/03/2002

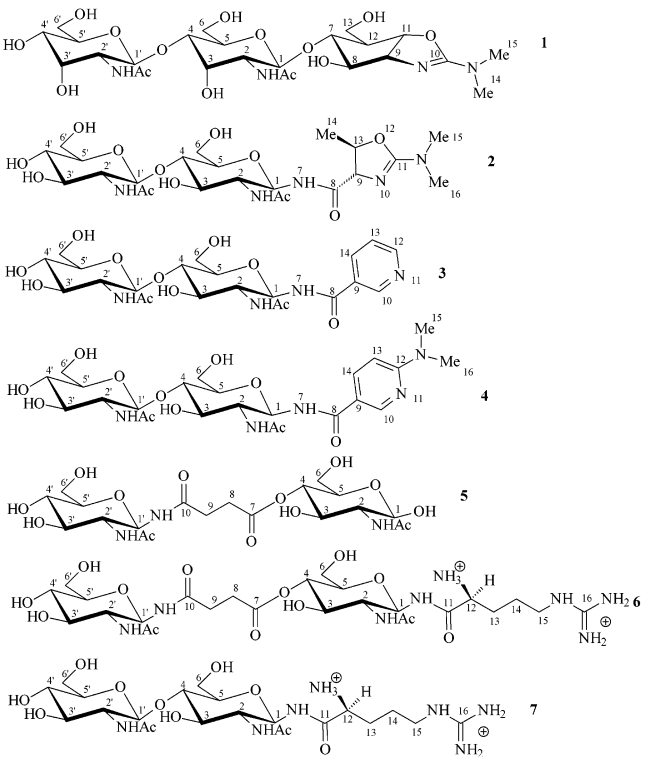

FIGURE 1. Structures of the hevamine inhibitor allosamidin (**1**) and the six analogues (**2**−**7**) examined in this work together with the numbering system in use.

analogy to the natural substrate chitotriose, whereby one sugar residue has been replaced by a succinamide group.

The analogues, given their structure, could be inhibitors of chitinases in general. However, in competitive enzyme assays using a Chitinase from *Hevea brasiliensis*,[6] only allosamidin (**1**) exhibited appreciable competition with the fluorogenic 4-methylumbelliferone glycosids of $GlcNAc_2$ and $GlcNAc_3$. Allosamidin (**1**) was also recently tested by Bokma et al.[7] with hevamine[8] and was found to be a competitive inhibitor with a K_i of 3.1 μM.[9] Despite this, the six analogues **2**−**7** may still exhibit inhibitory effects to some extent and may bind to hevamine, irrespective of their inhibitory properties in competitive enzyme assays. This aspect formed a secondary part of the NMR investigation of these compounds. There are an ever-growing number of NMR-based screening techniques encompassed by the broad classification of (bio)affinity NMR,[10,11] including diffusion-based[10] experiments and dipolar coupling (NOE)-based experiments such as (reverse) NOE pumping,[12,13] saturation transfer difference[14] (STD), and transfer-NOESY (trNOESY).[15,16] These experiments generally rely on the vastly different physical NMR properties of the much larger molecules to modulate the signals of the smaller, binding analytes; there is a heavy dependence on the experimental conditions—both the spectrometer performance and the sample properties—for success of the experiment. Accordingly, the compounds **1**−**7** were screened for their ability to complex to hevamine in solution using as screening probes trNOESY and 1-D and 2-D STD experiments in addition to assessing chemical shift changes in the ^{1}H and ^{13}C spectral ranges by HMQC.

Results and Discussion

^{1}H and ^{13}C NMR Assignments and Gross Structural Determination. The assignment of the proton NMR spectra of compounds **1**−**7** was far from trivial as many resonances were extensively overlapped, in particular, the pyranose ring protons**.** However, the spectrally distinct anomeric protons were, as expected, useful entry points into the spin systems, and the standard application of DQF-COSY, TOCSY, and HMQC experiments corroborated by the additional application of HMQC-TOCSY experiments provided the assignments of each sugar residue. HMBC spectra were acquired for both the assignment of the quaternary carbons and to substantiate the interresidue linkages. For example, in compounds **1**−**4**, the ring connections could be ascertained by the presence of H-1′, C-4 cross-peaks. For compounds **2**−**4**, a long-range coupling between H-1 and C-8 manifested itself to similarly provide that ring connectivity. The ^{1}H and ^{13}C chemical shifts and the vicinal coupling constants between H-1 and H-2, H-5 and H-6(*pro-S*), and H-5 and H-6(*pro-R*), respectively, of the compounds **1**−**7** are given in Tables 1 and 2.

For each of the carbohydrate units in all of the compounds examined, $^3J_{H\text{-}1,H\text{-}2}$ was ca. 8−9 Hz due to the axial trans orientations of both the H-1 and H-2 protons (or the H-1′ and H-2′ protons); i.e., each sugar unit—the *N*-acetylglucosamine residues in **2**−**7** and the *N*-acetylallosamine residue in **1**—was present as the β-anomer.

Conformational Analysis by NMR Spectroscopy and Molecular Modeling. Conformational preferences were assessed by the acquisition of the inter- and intraresidue NOEs to assess the spatial dispositions of the nuclei in compounds **1**−**7**. However, it is particularly prevalent in the application of NOESY to oligosaccharides that extensive overlap of the resonances renders the integration of the NOE cross-peaks problematic to such an extent that an rms value of the order of 0.5 Å was estimated for the uncertainty in these distance calculations. Therefore, in the present work, the NOE information was assessed in a semiquantitative manner but it was still necessary to convert the measured NOEs into spatial values to obtain a sufficiently precise determination of the structure of the compounds under study. Accurate interproton distances can be obtained from the nuclear cross-relaxation rates,[17] which are measurable from the initial build up rates of the NOE cross-peaks between dipolar-coupled protons. A uniform correlation time for all NOE interactions observed was assumed for

(6) Tata, S. J.; Beintema, J. J.; Balabaskaran, S. *J. Rubb. Res. Inst. Malaysia* **1983**, *31* (1), 35.
(7) Bokma, E.; Barends, T.; Terwisscha van Scheltinga, A. C.; Dijkstra, B. W.; Beintema, J. J. *FEBS Lett.* **2000**, *478*, 119.
(8) Terwisscha van Scheltinga, A. C.; Armand, S.; Kalk, K. H.; Isogai, A.; Henrissat, B.; Dijkstra, B. W. *Biochemistry* **1995**, *34*, 15619.
(9) Brameld, K. A.; Schrader, W. D.; Imperiali, B.; Goddard, W. A. *J. Mol. Biol.* **1998**, *280*, 913.
(10) Chen, A.; Shapiro, M. J. *Anal. Chem.* **1999**, *71*, 669A.
(11) Weimar, T. *Magn. Reson. Chem.* **2000**, *38*, 315.
(12) Chen, A.; Shapiro, M. J. *J. Am. Chem. Soc.* **2000**, *122*, 414.
(13) Chen, A.; Shapiro, M. J. *J. Am. Chem. Soc.* **1998**, *120*, 10258.
(14) Mayer, M.; Meyer, B. *Angew. Chem., Int. Ed. Engl.* **1999**, *38*, 1784.
(15) Clore, G. M.; Gronenborn, A. M. *J. Magn. Reson.* **1982**, *48*, 402.
(16) Clore, G. M.; Gronenborn, A. M. *J. Magn. Reson.* **1983**, *53*, 423.
(17) Solomon, I. *Phys. Rev.* **1955**, *99*, 559.

TABLE 1. ^{1}H Chemical Shifts (δ/ppm) and the Vicinal H,H Coupling Constants in the H1−H2 and H5−H6 Coupling Fragments of Compounds 1−7[a]

		1, 1′,7	2,2′,8	3,3′,9	4,4′,10	5,5′,11	6*R*/*S*,6′*R*/*S*, 12(*R*/*S*)	NHAc, 13	14	15/16	$^3J_{H1-H2}$ (Hz)	$3J_{H6S-H5}$ (Hz)	$3J_{H6R-H5}$ (Hz)
1	AllNAc	4.80	3.87	4.37	3.75	3.92	3.64/3.83	2.1			8.33	2.5	6.5
	AllNAc′	4.82	2.92	4.08	3.71	3.79	3.75/3.90	2.1			8.55	2.4	5.5
	allosamizoline	3.89	4.23	4.37	5.36	2.5	3.70/3.83		3.08	3.08	8.11	2.8	nd
2	GlcNAc	4.99	3.91	3.78	3.67	3.63	3.64/3.84	1.97			9.48	3.2	5.1
	GlcNAc′	4.60	3.76	3.58	3.49	3.49	3.77/3.92	2.07			8.09	2.1	5.3
	heterocyclic unit			4.64				4.04	1.41	2.95			
3	GlcNAc	5.29	4.02	3.84	3.70	3.69	3.70/3.87	1.98			9.63	1.9	4.9
	GlcNAc′	4.63	3.76	3.58	3.48	3.50	3.76/3.92	2.08			8.38	1.9	5.5
	heterocyclic unit				8.86		8.72	7.59	8.15				
4	GlcNAc	5.23	4.00	3.83	3.69	3.66	3.70/3.87	1.97			9.51	2.4	5.1
	GlcNAc′	4.63	3.77	3.56	3.49	3.50	3.77/3.94	2.08			8.18	2.2	5.2
	heterocyclic unit				8.39			6.66	7.81	3.08			
5(**1**-α)	GlcNAc	5.22	3.89	3.78	3.55	3.55	3.77/3.88	2.01			1.83	1.8	5.1
	Succ		2.65	2.55									
	GlcNAc′	5.05	3.82	3.59	3.48	3.50	3.74/3.87	2.04			9.73	1.7	5.1
5(**1**-*β*)	GlcNAc	4.77	3.67	3.54	3.56	3.55	3.77/3.88	2.01			7.7	1.8	5.2
	Succ		2.65	2.55									
	GlcNAc′	5.05	3.82	3.59	3.48	3.50	3.74/3.87	2.04			9.73	1.7	5.2
6	GlcNAc	5.15	3.95	3.87	3.50	3.51	3.73/3.87	2.01			9.25	2.3	5.1
	Succ		2.73	2.6									
	GlcNAc′	5.05	3.81	3.59	3.47	3.49	3.7073.84	2.04			9.71	2.3	5.2
	Arg						3.99	1.93	1.67	3.22			
7	GlcNAc	5.09	3.93	3.73	3.65	3.62	3.64/3.85	1.99			9.48	2.3	nd
	GlcNAc′	4.63	3.77	3.59	3.47	3.49	3.77/3.93	2.06			7.86	2.6	nd
	Arg						3.57	1.63	1.37	3.22			

[a] Estimated error for $^3J_{5,6} = \pm 0.2$ Hz; nd, not detected, because of severe signal overlap.

TABLE 2. ^{13}C Chemical Shifts (δ/ppm) of Compounds 1−7

		1, 1′,7	2,2′,8	3,3′,9	4,4′,10	5,5′,11	6,6′,12	NHAc, 13	14	15/16
1	AllNAc	104.1	56.7	73.2	81.2	76.8	65.2	26.3, 178.6		
	AllNAc′	104.7	57.1	74.3	70.5	77.8	65.1	26.3, 178.6		
	allosamizoline	89.3	84.8	69.1	90.6	55.6	63.6	165.5	42.2	42.2
2	GlcNAc	83.3	58.0	76.9	83.6	80.9	64.5	26.3/179.3		
	GlcNAc′	106.1	60.2	78.0	74.3	80.5	65.1	26.7/179.2		
	heterocyclic unit		169.1	86.2		181.6		76.4	25.4	41.6
3	GlcNAc	83.7	58.5	77.1	83.3	80.9	64.4	26.4/179.4		
	GlcNAc′	105.9	60.1	77.9	74.2	80.4	65.1	26.6/179.2		
	heterocyclic unit		173.6	133.3	152.2		156.7	128.8	140.9	
4	GlcNAc	83.8	58.5	77.2	83.4	80.7	64.5	26.4/179.5		
	GlcNAc′	106.0	60.1	78.0	74.2	80.4	65.1	26.6/179.2		
	heterocyclic unit		173.9	119.5	152.8		165.0	110.9	141.0	42.5
5(**1**-α)	GlcNAc	95.3	58.4	76.3	74.0	73.1	64.7	26.6/178.2		
	Succ	180.0	34.6	33.4	179.4					
	GlcNAc′	82.9	58.8	78.8	74.0	82.1	64.7	26.6/178.2		
5(**1**-*β*)	GlcNAc	99.5	60.9	76.3	74.0	73.1	65.1	26.6/178.2		
	Succ	180.0	34.6	33.4	179.4					
	GlcNAc′	82.9	58.8	78.8	74.0	82.1	65.1	26.6/178.2		
6	GlcNAc	83.0	58.6	76.6	74.1	nd[a]	64.6	26.6/179.6		
	Succ	178.3	34.6	33.5	180.0					
	GlcNAc′	83.1	58.9	78.8	74.1	82.2	65.1	26.6/179.6		
	Arg					175.0	57.4	32.4	27.9	44.9/161.4
7	GlcNAc	82.8	58.1	77.0	83.1	80.8	64.3	26.3/179.1		
	GlcNAc′	105.7	59.9	77.7	75.7	80.6	64.8	26.3/178.9		
	Arg					178.9	58.6	23.5	28.3	45.1/161.2

[a] nd: not detected because of severe signal overlap.

compounds **1**−**7** and under such an assumption, an unknown distance r_{ij} can be calculated from a known distance r_{kl} by using the following well-known relationship

$$r_{ij} = r_{kl}\left(\frac{\sigma_{kl}}{\sigma_{ij}}\right)^{1/6}$$

where σ_{ij} and σ_{kl} are the cross-relaxation rates between protons i and j and between protons k and l, respectively. However, it was not attempted to calculate exact distances from such an internal standard according to the above equation because of severe signal overlap and because of the uncertainty in the dynamic properties of different parts of the compounds, namely the carbohydrate and heterocyclic residues. Only the upper and lower bounds of interproton distances were estimated by calibration against known distances such as the distance between H-1 and H-3 (2.64 ± 0.01 Å) of the nonreducing residue of *N*-acetylglucosamine. Thus, the intensities of all the NOE cross-peaks at different mixing times were compared to the intensities of the NOE cross-peak

between H-1 and H-3 and assessed as follows. If the NOE cross-peak at a mixing time of 200 ms between a pair of protons was as strong as that between H-1 and H-3, then the distance between that interacting proton pair was assigned an upper bound of 2.8 Å. For a pair of protons with a weak NOE cross-peak at a mixing time of 200 ms, or with an intensive cross-peak at 400 ms, the distance between them was assigned an upper bound of 3.2 Å and a lower bound of 2.8 Å. An upper bound of 3.6 Å and a lower bound of 3.2 Å was assigned to the distance between proton pairs with weak NOE cross-peaks at a mixing time of 400 ms. Protons with barely observable NOE cross-peaks at mixing times of either 600 or 1000 ms were assumed to be separated by a distance constrained within the limits of 3.6−4.0 Å. Spin diffusion was excluded employing parallel 2D-ROESY NMR experiments.

Since the measured NOEs represent population-weighted averages of all participating conformers, NMR data alone therefore, can rarely define the structural composition of oligosaccharides unambiguously. Henceforth it follows that the conformational analysis of these compounds requires the additional aid of molecular modeling methods to complement the experimental NMR data. Thus, population-weighted average distances were calculated for the complete number of accessible conformations for compounds **1**−**7** and then compared to the experimentally observed NOE data. Each molecule was subjected to an extensive conformational search; grid search simulations were run to calculate relaxed potential energy (Φ, Ψ) maps. Population-weighted averages were then calculated from the conformational minima thus obtained employing weighting factors based on Boltzmann distributions[18] calculated from the relative energies. The distances in a system with N possible nondegenerate states can be calculated from

$$d = \sum_{i=1}^{N} f_i d_i$$

where f_i is a normalized weighting factor of state i, given by

$$f_i = \frac{q_i}{\sum_{i=1}^{N} q_i}$$

The quantity q_i is the individual partition function of state i, which is defined as

$$q_i = e^{-\Delta E/RT}$$

where ΔE is the energy difference between state i and the ground state, R the gas constant, and T the absolute temperature.

Concerning the conformational search of the hydroxymethyl group, only the *gt* and the *gg* orientations of the exocyclic portion were explicitly taken into account because the coupling constants $^3J_{\text{H5-H6-}proS}$ and $^3J_{\text{H5-H6-}proR}$ of **1**−**7** (cf. Table 1) show a rotameric distribution as *gg* ≥ *gt* ≫ *tg* (cf. Table 3). These results are in accordance with Nishida et al.,[19] who reported the corresponding conformations in *N*-acetylglucosamine and in water solution to be *gg*:*gt*:*tg* = ca. 60:40:0.[19] Thus, four combinations for the disaccharidic units in **1**−**4** and **7** were taken into account, namely *gg*−*gg*, *gg*−*gt*, *gt*−*gg*, and *gt*−*gt*; accordingly, these four initial configurations were considered. As reported previously, we found out that the shape of the potential energy surface is independent of the initial configuration of the hydroxymethyl group.[20]

TABLE 3. Determination of Rotameric Distributions of 1−7 Employing Conventional Equations I−III

general formula I−III: $1.3gg + 2.7gt + 11.7tg = J_{\text{H5-H6}S}$ (1)

$1.3gg + 1.5gt + 5.8tg = J_{\text{H5-H6}R}$ (2)

$gg + gt + tg = 1$ (3)

		$^3J_{\text{H6}S\text{-H5}}$ (Hz)[a]	$^3J_{\text{H6}R\text{-H5}}$ (Hz)[a]	rotameric distribution (%)		
				gg	*gt*	*tg*
1	AllNAc	2.5	6.5	46	48	4
	AllNAc′	2.4	5.5	55	38	5
	allosamizoline	2.8	nd	61	27	10
2	GlcNAc	3.2	5.1	54	31	14
	GlcNAc′	2.1	5.3	59	38	2
3	GlcNAc	1.9	4.9	64	34	1
	GlcNAc′	1.9	5.5	59	41	0
4	GlcNAc	2.0	5.1	62	36	2
	GlcNAc′	2.0	5.2	61	37	2
5(**1**-α)	GlcNAc	1.8	5.1	63	37	0
	GlcNAc′	1.7	5.1	63	38	−1
	GlcNAc	1.8	5.2	63	37	0
5(**1**-β)	GlcNAc′	1.7	5.2	63	38	−1
6	GlcNAc	2.3	5.1	60	35	5
	GlcNAc′	2.3	5.2	59	36	5
7	GlcNAc	2.3	nd			
	GlcNAc′	2.6	nd			

[a] Estimated error for $^3J_{5,6} = \pm 0.2$ Hz. nd: not detected because of severe signal overlap.

In the molecular modeling, a distance-dependent dielectric constant of 78 was used to implicitly consider the presence of the solvent water. To take this solvent effect into account, is particularly important in the modeling of carbohydrates due to their extremly strong tendency to form inter/intramolecular hydrogen bonds. We were aware of the difficulty of this approach in case of solvents which could be also be involved in hydrogen bonding. However, since the charge screening is the most important solvent influence, this approach should provide good results. Larwood et al.,[21] who studied among others the solvation effects on the conformational behavior of gellan with explicit and implicit inclusion of water, found out that there are no differences in the location of the minimum energy conformations around the glycosidic linkage, although there were differences in the orientation of some of the hydroxyl groups, and as expected, the hydroxyl groups of such residues were involved in hydrogen bonding with water molecules.[22]

We studied the solvation energy during the MD simulation in the presence of water molecules exemplary

(18) Atkins, P. W. In *Physikalische Chemie*, 1st ed.; VCH: Weinheim, 1988.

(19) Nishida, Y.; Hori, H.; Ohrui, H.; Meguro, H. *Carbohydr. Res.* **1987**, *170*, 106.

(20) Espinosa, J.-F.; Asensio, J. L.; Bruix, M.; J. Jimenez-Barbero *J. An. Quim. Int. Ed.* **1996**, *92*, 320.

(21) Larwood, V. L.; Howlin, B. J.; Webb, G. A. *J. Mol. Model.* **1996**, *2*, 175.

(22) Aida, M.; Sugawara, Y.; Oikawa, S.; Umemoto, K. *Int. J. Biol. Macromol.* **1995**, *17*, 3−4, 227.

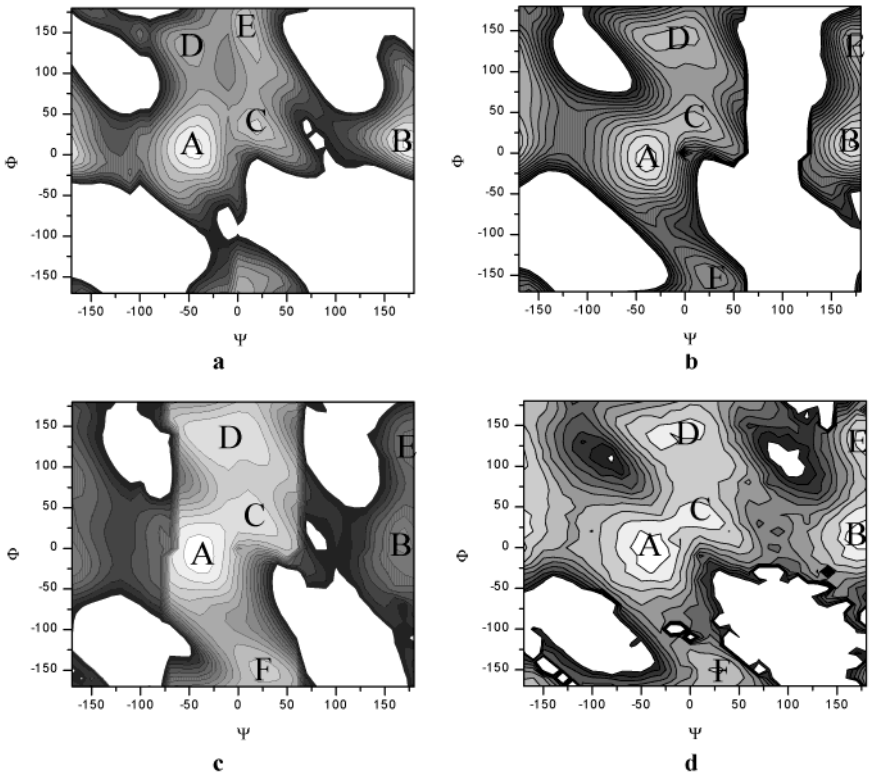

FIGURE 2. Contour plots a−d for compounds **1**−**4**, respectively, showing the relative populations about the torsional angles Φ ($H_{1'}-C_{1'}-O-C_4$) and Ψ ($C_{1'}-O-C_4-H_4$): (**A**) the global minimum; (**B**−**F**) other local minima.

for compound **3**: the six minima conformations around the glycosidic linkage of **3** (vide infra) were subjected to the MD simulation in a box of explicit water molecules, as described in more detail in the Experimental Section. The minimum energy conformations were restricted to aggregates; i.e., their relative geometry was not optimized. Therefore, only the interaction energy of compound **3** and water was calculated. These calculations proved very similar solvation energies to be present in all minimum energy conformations ($\Delta E_{solv} \sim \pm 1$ kcal/mol). From these results, it was concluded, that it is sufficient to consider the solvent in an implicit manner only along the calculation of the present disaccharide fragment, as long as the differences in the orientation of the hydroxyl groups in the two different models are considered correctly.

The Conformation of Compounds 1−4. The observed coupling constants (data not shown) and intraresidue NOE data are consistent with $^4C_1$ chair conformations being adopted by the two glucosamine and allosamine residues in each of the compounds **1**−**4**, and as such the dynamic conformational space is in essence defined by the torsional angles of the β-(1−4) glycosidic linkage, the β-(1′−4′) glycosidic linkage, and the amide (O−C_7 in **1**) linkage to the heterocyclic moiety. Contour plots of the conformer distribution about the glycosidic linkage $C_{1'}-O-C_4$ in **1**−**4** are depicted in panels a−d of Figure 2 with the positions of the global minimum, **A**, and the local minima, **B**−**F**, indicated.

Six local minimum conformers were obtained from the calculations. This result is in slight contrast to the report of Aida et al.,[22] who found chitobiose as a highly populated single conformer at the linkage domain, but it agrees with results of Espinosa et al.,[20] who indicated the existence of more than one populated region. Both groups observe the global minimum region A which is the usual conformation for the β-(1−4) glycosidic linkage.[23−25]

As expected, the torsional angles of the low energy conformers for compounds **2**−**4** are quite similar. The torsional angles Φ and Ψ of the low energy conformers both span a large range, a consequence of which is that it is difficult to define exactly, and to make comparisons between, the low energy conformers. The most striking difference between the conformers of **2**−**4** in comparison to **1** is the position of the local minimum conformer **F**. The underlying cause for the positional shift of this conformer in the conformational map is the *equatorial* orientation of H-3 in the *N*-acetylallosamine units of **1** in contrast to the *axial* orientation of H-3 in the *N*-acetylglucosamine units of **2**−**4**. Although all other minima **A**−**D** are similarly located in **1**−**4**, the local minimum **F** could not be clearly defined for **1** because of the steric hindrance between the *axial* C-3 hydroxyl group and the ring oxygen O-5′ in this conformation.

Each of the low energy conformations **A**−**F** thus found was set as a starting point for the next run of grid search simulations about the torsional angles Φ′ and Ψ′ for **1**, and χ1, χ2, and χ3 for **2**−**4**. As an example, in Figure 3 the contour plot of the torsional angles Φ′ and Ψ′ for allosamidin (**1**) is presented.

As expected, the positions of the local minima are not too dissimilar from the positions of the minima in panels

(23) Leeflang, B. R.; Vliegenhardt, J. F. G.; Kroon-Batenburg, L. M. J.; van Eijck, B. P.; Kroon, J. *Carbohydr. Res.* **1992**, *230*, 41.
(24) Dowd, M. K.; French, A. D.; Reilly, P. J.*Carbohydr. Res.* **1992**, *233*, 15.
(25) Engelsen, S. B.; Perez, S.; Braccini, I.; Herve du Penhot, C. *J. Comput. Chem.* **1995**, *16*, 1096.

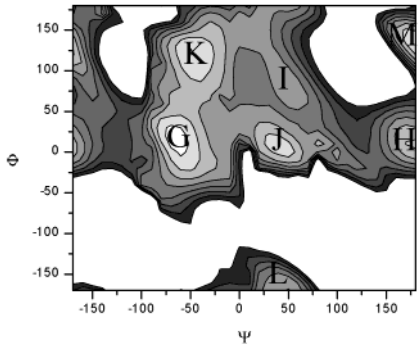

FIGURE 3. Contour plot showing the relative populations about the torsional angles Φ′ and Ψ′ of allosamidin (**1**) and indicating the positions of the minima **G**−**M**.

b−d of Figure 2, and as such the low-energy conformations about the glycosidic bonds of allosamidin (**1**), by comparison to compounds **2**−**4**, are therefore determined by the *equatorial* and *axial* orientations of H-3 and H-8, respectively. For allosamidin (**1**), six conformational families about the glycosidic $C_{1'}-O-C_4$ linkage and seven conformational families about the glycosidic C_1-O-C_7 linkage were calculated. Compounds **2**−**4** are also represented by six conformational families about the glycosidic $C_{1'}-O-C_4$ linkage. Regarding the torsional angles $\chi1$, $\chi2$, and $\chi3$: $\chi1$ has two local minima at ca. 0° and ca. 180° for the three compounds **2**−**4**, a trans conformation is highly favored for $\chi2$, and the high flexibility about $\chi3$ shows two local minima at 0° and 180° for **3** and **4** and three local minima at 60°, 120°, −60° for **2**. All these minima have been verified for compounds **2**−**4** by ab initio MO calculations. The calculated, and moreover expected, stretched orientation of the heterocyclic moiety for compounds **2**−**4** with respect to the pyranose ring was consistent with the NMR data in as far as no interresidual NOE between the middle *N*-acetylglucosamine residue and the heterocyclic ring could be measured. Overall, as a result of the calculations, 42 low energy conformations were found for allosamidin (**1**), 36 for compound **2**, and 12 for both compounds **3** and **4**.

Comparison of the theoretical NOEs calculated from the global energy minimum conformation to the experimental data quickly proved incongruous. For instance, a calculated internuclei distance between H-1′ and H-3 of 2.2 Å for the global minimum conformation **A** of compound **3** was not fully consistent with an observed medium-sized NOE. Thus by necessity, the experimental NOEs were treated as population-weighted averages of all likely participating conformers and population-weighted distances were calculated (vide supra). As an example, all 42 possible conformations for allosamidin (**1**) were included in the calculations with each conformer possessing an equal number of degeneracies with respect to rotation about either the hydroxy or hydroxymethyl groups. For each of the 42 conformations, the H−H interresidue distances were extracted and statistically weighted according to the Boltzmann population of the conformer. In Table 4, the interresidual NOEs for compounds **1**−**4**, are presented together with the weighted distances of their low energy conformers. In accordance with the NMR experiments, the temperature of the calculations was set at 313 K.

TABLE 4. Comparison of NMR Data (Intensity of Interresidual NOEs) and Population-Weighted Average Values for All Low-Energy Conformations of 1−4 Obtained by Force Field Calculations

compd	hydrogens	signal intensity[a]	avg distance (Å)
1	H-1′, H-4	vs	2.60
	H-1′, H-3	vs	2.62
	H-1′, H-5	nd	4.32
	H-1′, H-6a	w	4.11
	H-1′, H-6b	w	4.55
	H-1, H-8	nd	3.15
	H-1, H-13a	w	4.48
	H-1, H-7	s	3.01
2	H-1′, H-4	s	2.99
	H-1′, H-3	s	2.88
	H-1′, H-5	s	3.29
	H-1′, H-6b	nd	3.69
	H-2′, H-6b	nd	3.83
3	H-1′, H-4	vs	2.82
	H-1′, H-3	s	3.11
4	H-1′, H-4	vs	2.85
	H-1′, H-3	s	3.20

[a] vs, very strong (<2.8 Å); s, strong (2.8−3.2 Å); m, medium (3.2−3.6 Å); w, weak (3.6−4 Å); and nd, not detected.

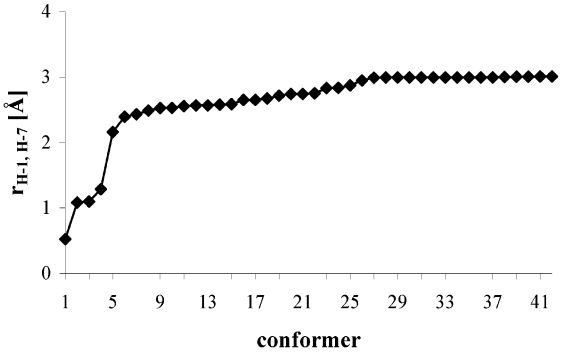

FIGURE 4. Population-weighted contribution to the internuclei distance between H-1 and H-7 for each of the 42 low-energy conformations of allosamidin (**1**). Overall, the population-weighted average value was calculated as 3.01 Å, which compares favorably to the experimentally determined range of 2.8−3.2 Å. The global minimum conformation 5 ($r_{H-1,H-7}$ = 2.52 Å) contributes up to 34% of the (0.83 C) averaged value.

The comparison of the NOEs that should result from the internuclei distances averaged from all the participating low energy conformers of **1**−**4** clearly fit the experimental data well. Although the distances between the interresidual protons are dominated by the global minimum, the fit is better when all local minima are taken into account. For example, the global minimum of **1** (Φ, −6.8°; Ψ, −44.4°; Φ′, −9.5°; Ψ′, −42.6°) is populated by up to 34% and the distance in this conformer between H-1 and H-7 is 2.52 Å, which should result in a measurably very strong NOE. However, the experimental NOE is only categorized as strong, implying that the actual distance is constrained within the range of 2.8−3.2 Å, a result that compares most favorably to the population-weighted average value of 3.01 Å. In Figure 4, the population-weighted contributions to the internuclei distance between H-1 and H-7 for each of the 42 low energy conformations of allosamidin (**1**) are displayed.

In essence, while the conformational behavior of the compounds **1**−**4** in solution is dominated by from two to six principle conformations, there are still many other low-energy conformers of lower population that contrib-

TABLE 5. Torsional Angles about the Glycosidic/Heterocyclic Moiety Linkages and the Corresponding Relative Energies of the Conformational Families

	minimum about Φ and Ψ	Φ and Ψ (deg)	rel energy (kcal/mol)	minimum about Φ′ and Ψ′/χ1, χ2, χ3	Φ′ and Ψ′/χ1, χ2, χ3 (deg)	rel energy (kcal/mol)
1	A	−9, −46	0	G	−9, −46	0
	B	12, 173	0.88	H	9, 177	0.77
	C	35, 19	3.50	I	86, 50	2.17
	D	136, −49	1.20	J	5, 43	0.4
	E	167, −15	1.36	K	148, −46	1.04
	F	−177, −154	5.33	L	−165, 48	1.73
				M	136, 177	0.23
2	A	−9, −4	0	G	−25, 171, 93	0
	B	12, 173	0.19	H	179, −177, 129	1.42
	C	37, 7	1.94	I	179, −173, −65	1.72
	D	137, −31	2.10	J	−21, 178, −60	0.11
	E	−150, 28	3.72			
	F	−127, 180	1.95			
3	A	−8, −40	0	G	−17, 173, 0	0
	B	13, 173	0.31	H	−17, 173, 180	
	C	36, 8	2.05	I	179, 173, 0	1.63
	D	136, −30	2.12	J	179, 173, 180	
	E	−150, 27	3.80			
	F	127, 180	2.06			
4	A	−8, −40	0	G	−17, 173, 0	0
	B	13, 173	0.20	H	−17, 173, 180	
	C	36, 13	2.08	I	179, 173, 0	1.55
	D	145, 2	2.29	J	179, 173, 180	
	E	−150, 27	3.67			
	F	126, 180	1.94			

ute significantly to the averaged result. The torsional angles of the principle conformers are summarized in Table 5; the six conformational families of **2**−**4** about the glycosidic linkage $C_{1'}$−O−C_4 are depicted in Figure 5; and the conformational behaviors about the linkage to the heterocyclic moiety for **2** and **3** are depicted in Figure 6.

Concerning the conformational preference of allosamidin (**1**), it was interesting to compare the free conformations found here in solution with the conformation of allosamidin (**1**) found from the X-ray crystal structure determination of the hevamine−allosamidin complex.[8] In Figure 7, the X-ray structure of allosamidin (**1**) from the hevamine−allosamidin complex and the calculated global minimum conformation of **1** are overlaid for comparative purposes. It is clear that the conformations of the glycosidic bond as defined by Φ and Ψ belong to the same conformational family for both structures; however, the conformations about Φ′ and Ψ′ of the free and complexed conformers are markedly different. The conformation of the complexed allosamidin (**1**) as determined by X-ray analysis was not obtained at all as a calculated local minimum conformer; therefore the complexed conformation has to be a result of stabilization by hydrogen bonds and hydrophobic interaction with the protein. The deformation energy of bound allosamidin compared to the free analogon was calculated to be about 5 kcal/mol.

The Conformation of Compounds 5 and 6. The syntheses, together with some of the conformational aspects, of compounds **5** and **6** have been published recently.[5] It was shown that these compounds are highly flexible and that the overall conformation of the pseudotrisaccharides is determined by χ5. Consistent with these findings, calculations provided one anti and two gauche orientations with respect to χ5. Each of these occurs in one of four low-energy conformations with respect to χ4 and χ6 (see Figure 8). The χ5 anti orientation results in an extended linear disposition (**A**) whereas the gauche conformers lead to folded conformations (**B** and **C**). The AMBER force field calculations also revealed that Φ is favored by orientations of ca. −10° and ca. 170° (see Figure 9).

Since the global minimum conformation of **5** is folded, strong interresidue NOEs might be expected to result. However, the population-weighted averaged proton−proton interresidue distances of all calculated conformations was found to exceed 3.6 Å; thus, despite the fact that the calculated global minimum conformation should yield strong NOE contacts (e.g., between H-6a′ and H-8, H-4 and H-8, and H-4 and H-9), NOEs were not detected between the nonreducing and the reducing *N*-acetylglucosamine residues. This result is in accordance with the assumption that several conformations again exist in equilibrium and furthermore, the number of conformations for compound **5** can be classified into 12 basic conformational families with respect to the flexible bonds χ4, χ5, and χ6. The conformational families of **5** are presented in Table 6. Rotation about either χ7 or χ8 increases the conformational flexibility further. In the contour plot (Figure 10), the four local minimum conformations are displayed. The global minimum **I** with χ7 within 50−100° and χ8 ca. −40° is also the broadest; i.e., the system is highly flexible in this region.

Compound **6** displays, with respect to the pseudotrisaccharide unit, essentially the same conformational behavior as **5**. The C-7 amide group in **6** favors the *E*-configuration. The four low-energy conformers of **6** which are found by energy minimization of ϕ and χ4 are depicted in Figure 11. As expected, NOE contacts could only be observed between methylene groups, indicating that the arginine chain is in a stretched conformation.

The Conformation of Compound 7. The conformational behavior of compound **7** about the glycosidic linkages by comparison is similar to the conformational behavior of compounds **2**−**4**, implying that the conformational preferences about the glycosidic linkages are not influenced by the heterocyclic moiety to any signifi-

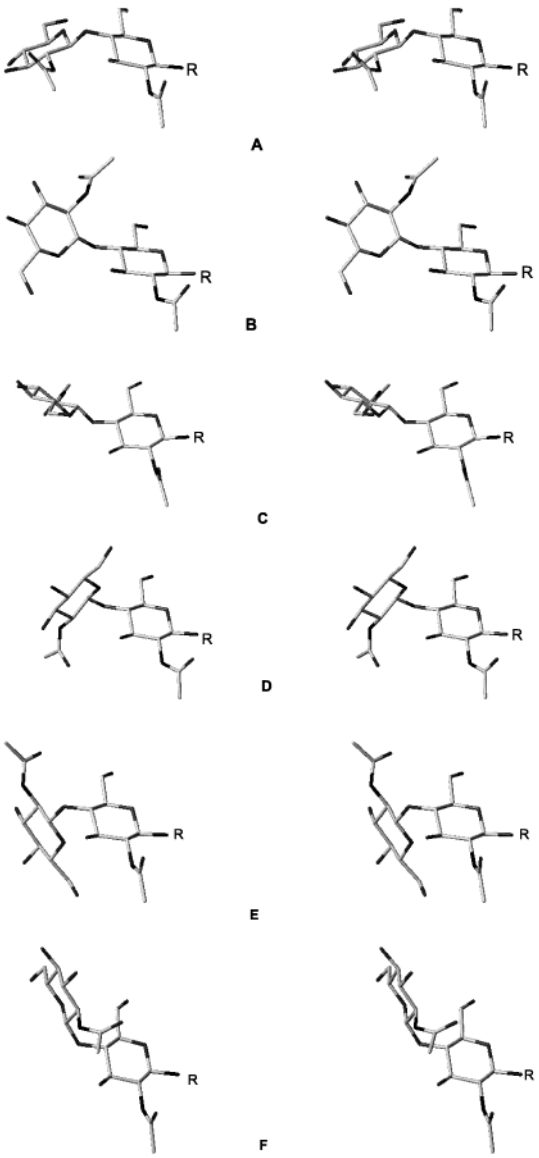

FIGURE 5. Stereoview of the conformational families **A**−**F** of **2**−**4** about the glycosidic linkages. R represents the heterocyclic moiety.

cant extent. The conformational minima **A**−**F**, presented in Table 7, are similar to the conformational minima of compounds **2**−**4**. Experimental NOE enhancements as well as calculated population-weighted average distances are presented in Table 8.

The conformational behavior of the arginine residue is also comparable to the behavior of this residue in compound **6**.

Analysis of the Binding of Compounds 1−7 to Hevamine by NMR. Compounds **1**−**7** were all treated in solution with hevamine and subjected first to tr-NOESY experiments. Given the lack of inhibition, it was not surprising that trNOESY cross-peaks were not observed for compounds **2**−**7**. However, since allosamidin (**1**) is known to be an inhibitor with K_i ∼3.1 μM at pH 4.2,[9] trNOESY cross-peaks should be observable for this compound. However, under the experimental conditions that were employed here, none were forthcoming. It could therefore be assumed that at physiological conditions (pH ∼7), the reduced K_i and k_{off} prevent observation of

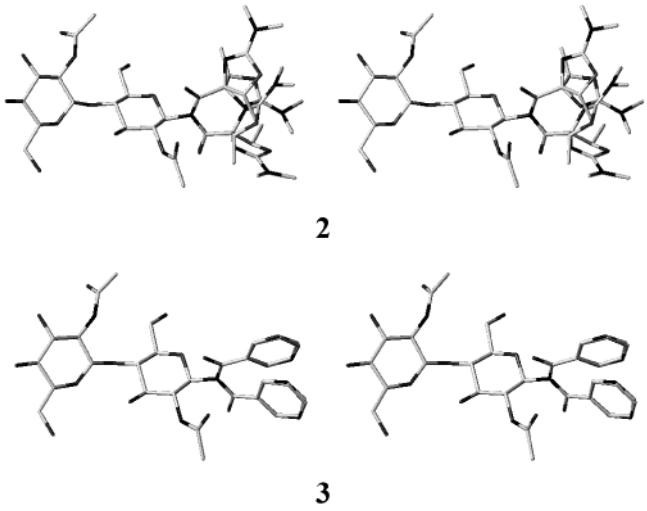

FIGURE 6. Stereoview of the conformational families of **2** and **3** with respect to χ1, χ2, and χ3. The conformational behavior of **4** is similar to that of **3**.

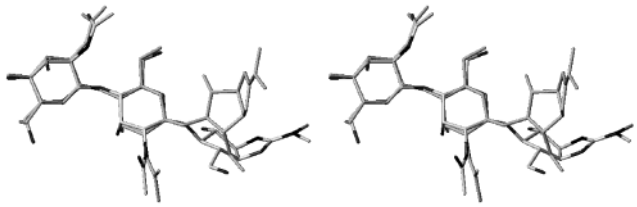

FIGURE 7. Stereoview overlays of the X-ray crystal structure (single colored framework) of allosamidin (**1**) from the hevamine−allosamidin complex and the calculated global minimum solution-state conformation of allosamidin (**1**) (framework containing atomic coloring).

TABLE 6. Conformational Families of Compound 5 with Respect to χ4, χ5, and χ6 (χ1 ca. −10°, χ7 within 70−110°, and χ8 ca. −40° for All Conformational Families)

conform	χ4 (deg)	χ5 (deg)	χ6 (deg)	rel energy (kcal/mol)
1	−43	−53	−70	2.17
2	−48	−60	100	1.83
3	−49	93	−100	0
4	−45	99	110	2.74
5	69	−94	−120	1.25
6	73	90	70	9.84
7	70	95	−120	8.45
8	71	−90	70	10.69
9	−172	66	80	9.31
10	176	77	−120	10.17
11	175	−80	−110	10.85
12	179	−90	80	11.5

NOESY cross-peaks. In addition, the success of these NOE-based experiments in general is heavily dependent on experimental factors; not just instrumental factors pertaining to the instrument performance, but also to the sample properties and the physical NMR properties of both the ligand and in particular, the substrate. The experimental conditions such as the field, solution viscosity etc., have a direct effect on the performance of the experiment by influencing such critical parameters as the cross relaxation rates,[14,15] molecular correlation times,[10,11,13,15,16] relaxation times,[10] etc. In terms of the sample chemistry itself, turnover rates[14] in addition to binding constants[10,14] and the relative proportions of the

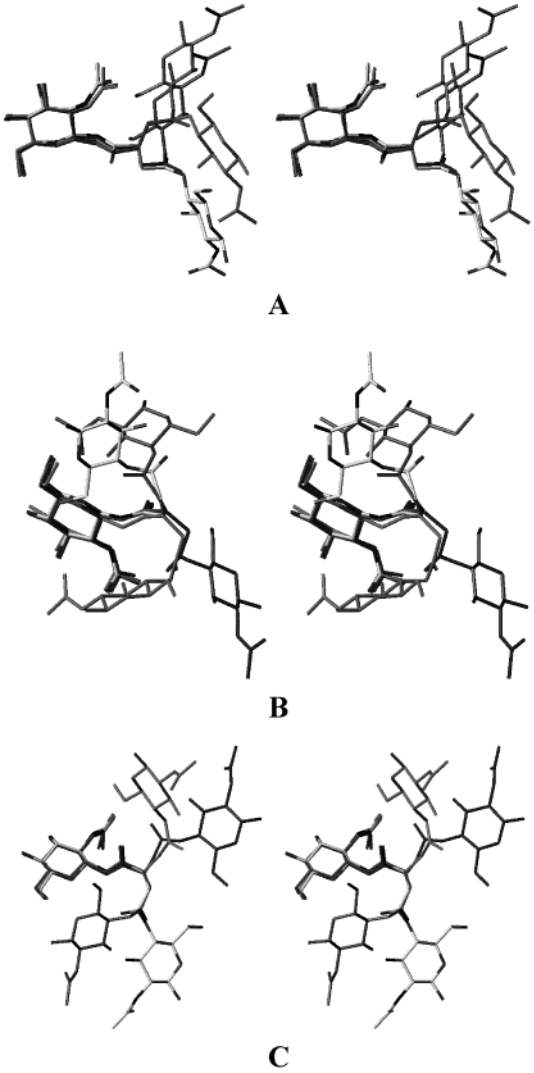

FIGURE 8. Stereoview of the low energy conformations of **5**,[5] four each minimized for χ4 and χ6 in one anti (A, $\chi5 = 180°$) and two gauche (B, $\chi5 = 60°$; C, $\chi5 = -60°$) conformations.

TABLE 7. Torsional Angles at the Glycosidic Linkages and the Corresponding Relative Energies of the Conformational Families A−F for Compound 7

conform	Φ, Ψ (deg)	rel energy (kcal/mol)
A	−8, −39	0
B	12, 173	2.5
C	35, 15	1.63
D	134, −31	1.9
E	126, 179	1.77
F	150, 29	3.63

interacting species[10,14] also have a determinate effect on the outcome of the experiment.

For the next attempt at screening the compounds for binding to hevamine, the more versatile and robust STD experiments[14] were applied and both 1-D as well as 2-D STD-TOCSY experiments were employed. It was again found that none of the compounds **1**−**7**, including allosamidin (**1**), under these experimental conditions was sufficiently bound to hevamine to effect a measurable response under the described conditions, the aforementioned caveats notwithstanding. Thus, neither STD or trNOESY was sufficiently sensitive to elicit a response

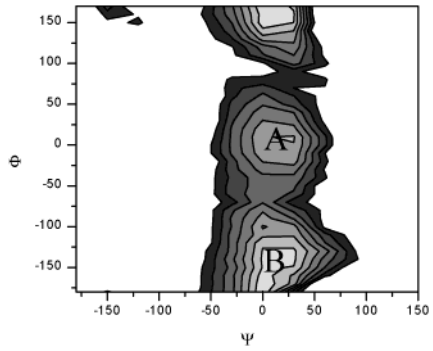

FIGURE 9. Contour plot of Φ and Ψ for compound **5**.

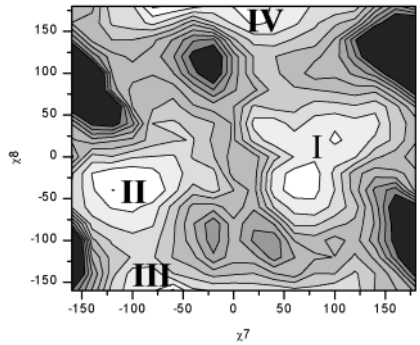

FIGURE 10. Contour plot of torsional angles χ7 and χ8 of compound **5**.

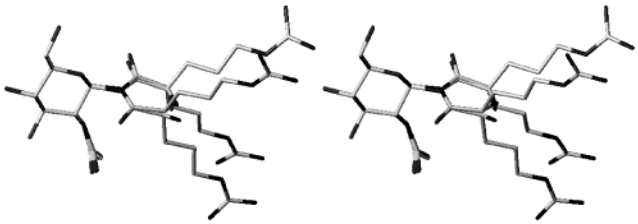

FIGURE 11. Stereoview of the low energy conformers of **6** representing the energy minima of Φ and χ4. The nonreducing *N*-acetylglucosamine end unit and the succinamide portion are not depicted.

TABLE 8. Comparison of NMR Data (Intensity of Interresidual NOEs) and Calculated Population-Weighted Average Distances for the Low-Energy Conformations A−F of Compound 7

hydrogens	exptl NOE[a]	calcd distance (Å)
H-1, H-4′	s	2.86
H-1, H-3′	s	3.13
H-1, H-5′	w	3.61
H-1, H-6a′	nd	4.43
H-1, H-6b′	nd	3.76

[a] s, strong (2.8−3.2 Å); w, weak (3.6−4 Å); and nd, not detected.

for complex formation for these compounds as the binding to hevamine is either too weak or nonexistent despite STD being touted a very responsive probe.[14]

A final approach was to simply examine whether chemical shift changes were discernible in the ^{1}H and the ^{13}C spectra of the compounds **1**−**7** between solutions not containing hevamine and subsequently those to which hevamine had been added. Since ^{1}H chemical shifts can be somewhat sensitive to the environment, the results were needed to be substantiated by the acquisi-

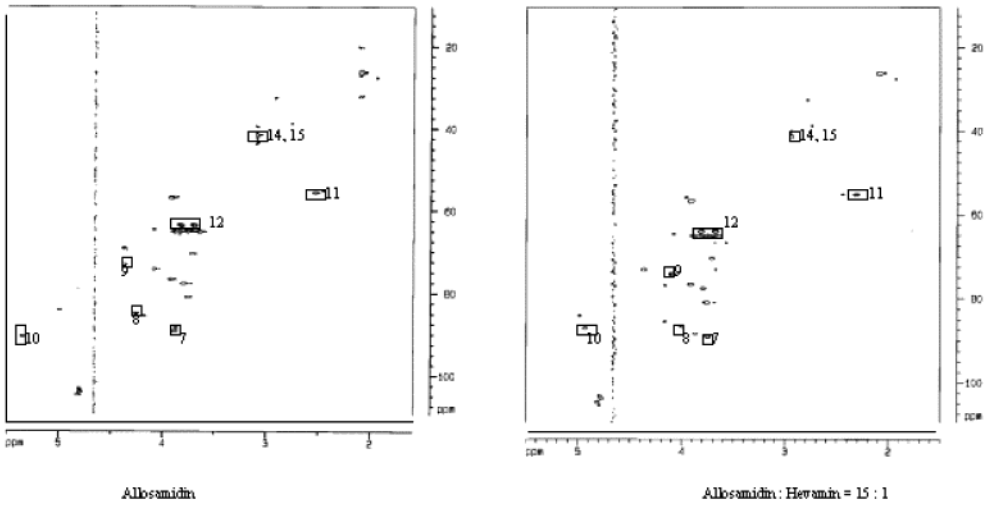

FIGURE 12. HMQC spectra of allosamidin (**1**) (left) and the hevamine−allosamidin complex 1:15 (right).

TABLE 9. ^{1}H and ^{13}C Chemical Shift Changes in ppm for Allosamidin (1) Following the Addition of Hevamine

atom label	^{1}H	^{13}C	atom label	^{1}H	^{13}C
7	−0.13	−0.2	11	+0.42	−3.5
8	−0.28	+1.8	12	−0.19	−0.4
9	−0.25	+5.1	13	−0.03	+0.4
10		+1.7	14, 15	−0.15	−0.8

tion of ^{13}C spectra. Due to the complexity and overlap of the spectra, and in particular the low sensitivity of carbon at the concentrations employed, it was appropriate to obtain this information by acquiring HMQC spectra to overcome these experimental shortcomings and ensure at the same time the correct assignment of the signals. Compounds **2**−**7** did not reveal any significant changes in either the ^{1}H or ^{13}C spectral regions and only allosamidin (**1**) displayed significant chemical shift changes. Moreover, these changes were restricted to the allosamizoline ring. In Figure 12, the HMQC spectra of allosamidin (**1**) and the hevamine-allosamidin complex are presented with selected chemical shift changes quantitatively listed in Table 9.

Since significant chemical shift variations were only observed in the allosamizoline moiety, it can be inferred that the van der Waals forces between allosamidin (**1**) and hevamine must be strongest in this region of the allosamidin (**1**) structure. This result is in agreement with those of Terwisscha van Scheltinga et al.[8] who also reported close contacts between the allosamizoline group and hevamine and is consistent with the distinct divergence between the conformational preferences determined by X-ray analysis and inferred by the calculations (vide supra). The large shifts to lower field by C-9 (+5.1 ppm) and C-10 (+1.7 ppm) could be the result of a strong interaction between the Asp125 residue of hevamine and the nitrogen of the allosamizolin ring. A shift also to lower field by C-8 (+1.8 ppm) could result from a hydrogen bond between the C-8 hydroxyl and the NH of Trp255. The shifts to lower frequency for all of the hydrogens bar H-11 could result from the hydrophobic contacts between the inhibitor and the Trp255, Tyr183, and Tyr6 residues. Finally, the substantial shift to lower field by H-11 (+0.42 ppm) in tandem with the shift to higher field by C-11 (−3.5 ppm) is possibly indicative of a proportionate steric compression effect which may actually imply that allosamidin (**1**) is strongly bound to hevamine, albeit in a highly localized manner. Thus, the NMR results were finally found to be consistent with the biochemical results which showed that only allosamidin (**1**) acted as a competitive inhibitor.

Conclusions

It has been amply demonstrated that conformational analysis of the manner performed on the compounds examined here is insufficiently addressed by NMR alone and that an accompanying molecular modeling study is required. For although a clear global minimum can be determined, the experimentally obtained spatial information agreed well with the computational results only if the weighted average of the participating conformers was considered. That is, the calculated distances were required to be statistically weighted averages with respect to the conformer populations of the various contributing conformers as determined by their calculated relative energies. Using this approach, the NMR data and molecular modeling results were no longer asynchronous and as such it was evident that the compounds adopt a number of conformations that originate from more than one conformational family.

The mixtures of allosamidin (**1**) and the compounds **2**−**6** with hevamine were all subjected to trNOESY, STD, and HMQC NMR experiments to determine the state of complex formation. Of note is the fact that the apparent weak binding of the known inhibitor allosamidin (**1**) under the experimental conditions employed precluded a response from the NMR probes often utilized for such screenings, namely trNOESY and STD. Compounds **2**−**6** failed to show any indication at all of complex formation for all three NMR techniques, consistent with their lack of inhibitory effects. Only allosamidin (**1**) showed significant signal shifts in the ^{1}H and ^{13}C spectral regions pertaining to the allosamizolin ring, thus confirming the robustness of HMQC in eliciting a response relating to a recognized interaction. The implications for research endeavors using various affinity NMR techniques for the screening of combinatorial libraries are self-evident from these results.

Currently, we are extending our experimental work and one aspect is to use the calculated low-energy conformers as initial structures for docking studies with hevamine. The combined results could be used for describing the structure of the ligands and potential inhibitors both in the free state and in the enzyme−inhibitor complex.

Experimental Section

NMR spectra were acquired using either a Bruker ARX 300 NMR spectrometer operating at 300 and 75 MHz (for ^{1}H and ^{13}C, respectively, and for compounds **2**−**7**) or a Bruker DMX 600 NMR spectrometer operating at 600 and 150 MHz (for ^{1}H and ^{13}C, respectively, and for compounds **1** and **5**). Spectra were recorded at 313 K without sample spinning using the HDO signal as internal reference (4.61 ppm). Data acquisition and processing were performed using Bruker XWINNMR software. For the assignment of the ^{1}H and ^{13}C signals, COSY, phase-sensitive HMQC,[26] HMBC,[27] as well as HMQC-TOCSY[28] experiments were performed. NOESY (mixing times 200, 400, 600, and 1,000 sec), ROESY (mixing time 250 ms, spin-lock field 2−3 kHz), and TOCSY[29] (mixing time 80 ms, spin-lock field 8 kHz) experiments were all recorded in phase-sensitive mode with a relaxation delay of 2 s. For all 2-D spectra, a total of 2 k data points in t_2 and 512 data points in t_1 were recorded. Suppression of the residual HDO signal was accomplished by presaturation. For 2-D trNOESY[15,16] experiments (mixing times 150, 300, and 600 ms), the HDO signal was suppressed by low-power presaturation during both the relaxation and mixing times. The total relaxation delay was 1.2 s. For 1-D STD experiments,[14] saturation transfer was accomplished by the use of 39 selective 1K Gaussian 90° pulses of duration 50 ms and spacing of 1 ms. The protein envelope was irradiated at either 1.2 or 7.2 ppm (on resonance for both) and then 20 ppm (off resonance). Subtraction was effected by phase cycling. Saturation times of 0.5, 1.0, 1.5, and 2 s were utilized. The relaxation delay was set to 1 s for **1** and 4 s for **3** and **5**. TOSCY and STD-TOCSY spectra were recorded with 256 increments and 32 transients using a MLEC 17 spin-lock field of 60 ms at 7.5 kHz. The relaxation delay was set to 4 s for **1** and to 12 s for **3** and **5**.

For the calculation of the rotameric population of the *gg*, *gt*, and *tg* conformers around the C5−C6 bond, the conventional equations I−III[30−32] were employed (cf. Table 3).

Molecular Modeling calculations were performed on either a Silicon Graphics Oxygen R5000 or a Silicon Graphics Origin 24 x R10000 workstation. All calculations employed the AMBER[33] force field routine implemented into the SYBYL 6.4[34] program. Based on GLYCAM-93[35] parameters, a new set of parameters was developed that is consistent with AMBER (details to be published elsewhere). Torsional angles at the glycosidic and other interresidual linkages are defined as follows (cf. Figure 1): Φ ($H_{1'}-C_{1'}-O-C_4$) for **1**−**4** and **7** and ($H_{1'}-C_{1'}-N-C_{10}$) for **5** and **6**; Ψ ($C_{1'}-O-C_4-H_4$) for **1**−**4** and **7** and ($C_{1'}-N-C_{10}-O$) for **5** and **6**; Φ' ($H_1-C_1-O-C_7$) and Ψ' ($C_1-O-C_7-H_7$) for **1**; χ1 ($H_1-C_1-N_7-C_8$), χ2 ($C_1-N_7-C_8-C_9$), and χ3 ($N_7-C_8-C_9-N/C_{10}$) for **2**−**4**; χ4 ($N-C_{10}-C_9-C_8$), χ5 ($C_{10}-C_9-C_8-C_7$), χ6 ($C_9-C_8-C_7-O$), χ7 ($C_8-C_7-O-C_4$), and χ8 ($C_7-O-C_4-H_4$) for **5** and **6**; χ9 ($H_1-N-C_{11}-C_{12}$), χ10 ($N-C_{11}-C_{12}-C_{13}$), and χ11 ($C_{11}-C_{12}-C_{13}-C_{14}$) for **6** and **7**.

At the beginning of the calculations, the glycosidic bond angles were fixed at 117° and the pyranose rings were treated as rigid $^4C_1$ conformation; similarly, the torsional angles ($O-C_5-C_6-OH$) and ($O-C_{5'}-C_{6'}-OH$) were fixed at 60° or −60°, corresponding to the *gt* and *gg* energy minimum conformation. Furthermore, the bond angles $C_{1'}-O-C_4$ and C_1-O-C_7 in **1**, $C_{1'}-O_{1'}-C_4$ and $C_1-N_7-C_8$ in **2**−**4**, and $C_{1'}-N-C_{10}$ and C_7-O-C_4 in **5** and **6** were set to 117°. 1,4-Interactions were scaled by a factor of 0.83, and a cutoff of nonbonding interactions at 12 Å was applied.

Simulation of 3 in a Box of Water. All six minima conformations around the glycosidic linkage of compound **3** were subjected to the MD simulation in a box of water molecules. The MD simulation was done at 300 K. First, the conformers were solvated using the XFIT algorithm of the SYBYL program. Within this algorithm the water molecules were placed randomly around the conformers avoiding any steric overlap. Cutoffs were employed for the nonbonding interactions up to 12 Å, since periodic boundary conditions were required to contain the water molecules. As the result, each system contained 1000 water molecules. The studied conformers were kept fixed during the whole simulation. The system was brought to equilibrium for 50 ps, and then finally, a 50 ps simulation was used for the analysis: coordinates and energies were stored every 50 fs.

Compounds **2**−**7** were synthesized as described previously.[4,5] All NMR samples were prepared using 1−5 mg of material which was lyophilized twice from 1 mL of D_2O prior to being taken up in 0.7 mL of D_2O followed by degassing in situ by aeration with argon for 30 min. For complexation studies, sufficient quantity of hevamine was added to the NMR solution to result in a ligand-to-enzyme molar ratio of 15:1.

Acknowledgment. This work was supported by EU Grant No. BIO4-CT-960670. Financial support from the Studienstiftung des deutschen Volkes is gratefully acknowledged (scholarship to A.G.). M.G.P. acknowledges partial support by the Fonds der Chemischen Industrie.

JO0163703

(26) Bax, A.; Subramanian, S. *J. Magn. Reson.* **1986**, *67*, 565.
(27) Wilker, W.; Leibfritz, D.; Kerssebaum, R.; Bermel, W. *Magn. Reson. Chem.* **1993**, *31*, 287.
(28) Domke, T. *J. Magn. Reson.* **1991**, *95*, 174.
(29) Otter, A.; Hindsgaul, O.; Bundle, D. R. *Carbohydr. Res.* **1995**, *275*, 381.
(30) Manor, P. C.; Saenger, W.; Davies, D. B.; Jankowski, K.; Rabczenko, A. *Biochim. Biophys. Acta* **1974**, *340*, 472.
(31) Wu, G. D.; Serianni, A. S.; Baker, R. *J. Org. Chem.* **1983**, *48*, 1750.
(32) Nishida, Y.; Hori, H.; Ohrui, H.; Meguro, J. *J. Carbohydr. Chem.* **1988**, *7*, 239.
(33) Cornell, W. D.; Cieplak, P.; Bayly, C. I.; Gould, I. R.; Merz, K. M.; Ferguson, D. M.; Spellmeyer, D. C.; Fox, T.; Caldwell, J. W.; Kollman, P. A. *J. Am. Chem. Soc.* **1995**, *117*, 5179.
(34) SYBYL Molecular Modeling Software, Version 6.4, TRIPOS, Inc., St. Louis, MO, 1997.
(35) Woods, R. J.; Dwek, R. A.; Edge, C. J.; Fraiser-Reid, B. *J. Phys. Chem.* **1995**, *99*, 3832.